POLITECNICO DI TORINO
Repository ISTITUZIONALE

Conformation-based Molecular Memories for Nanoscale MemComputing

Original
Conformation-based Molecular Memories for Nanoscale MemComputing / Ardesi, Y., Mo, F., Spano, C.E., Ardia, G., Piccinini, G., Graziano, M.. - ELETTRONICO. - (2023), pp. 694-697. (2023 IEEE 23rd International Conference on Nanotechnology (NANO) Jeju City, Korea, Republic of 02-05 July 2023) [10.1109/NANO58406.2023.10231199].

Availability:
This version is available at: 11583/2981539 since: 2023-09-08T08:42:30Z

Publisher:
IEEE

Published
DOI:10.1109/NANO58406.2023.10231199

Terms of use:

This article is made available under terms and conditions as specified in the corresponding bibliographic description in the repository

Publisher copyright
IEEE postprint/Author's Accepted Manuscript

©2023 IEEE. Personal use of this material is permitted. Permission from IEEE must be obtained for all other uses, in any current or future media, including reprinting/republishing this material for advertising or promotional purposes, creating new collecting works, for resale or lists, or reuse of any copyrighted component of this work in other works.

(Article begins on next page)

30 October 2026

Conformation-based Molecular Memories for Nanoscale MemComputing

Yuri Ardesi*‡, Fabrizio Mo*‡, Chiara Elfi Spano*, Gianmarco Ardia*,
Gianluca Piccinini* and Mariagrazia Graziano†§
*Department of Electronics and Telecommunications, Politecnico di Torino, Torino 10129, Italy
†Department of Applied Science and Technology and Telecommunications, Politecnico di Torino, Torino 10129, Italy
‡The two authors contributed equally to this work
§Corresponding author e-mail: mariagrazia.graziano@polito.it

***Abstract*—We investigate the use of endohedral fullerenes and 6-(Ferrocenyl)hexanethiol cation as molecular non-volatile memory devices. We demonstrate stable encoding of the information in the geometry and dipole moment of these molecules. The write operation can be performed with external programming electric fields that drive the switching of the molecule conformation. The read operation can be performed by reading the dipole moment through the generated electric fields. Moreover, the dipole moment encoding enables the integration of proposed memories with molecular Field-Coupled Nanocomputing logic. The capability to realize compatible and purely molecular memory and logic devices paves the way for molecular MemComputing, with new possibilities for nanoscale computing paradigms.**

I. Introduction

Molecular computing is one of the most attractive proposals for future digital electronics. The nanometric size of molecules enables the realization of highly dense devices for low power consumption at ambient temperatures [1], [2].

While the research community is pushing toward realizing devices with the smallest size, researchers are also studying architectural techniques to boost the speed of future processors. In particular, MemComputing, sometimes referred to as Logic-in-Memory [3]–[5], is one of the most effective paradigms. MemComputing bypasses the fetching operation by inserting logic in the memory array, thus permitting fast logic operations on memory data. Fig. 1(a) shows a basic example of a MemComputing cell: the logic device performs the comparison between an input (x) and a memory bit (M) through the XOR operation. Fig. 1(b) shows the MemComputing XOR operation applied to a memory array, where the stored 32-bit word (M) is compared with a specific input pattern (x). The complexity is increased w.r.t. a standard memory, yet, the fast access of the memory permits reducing the power consumption [6].

This work investigates the implementation of highly miniaturized molecular MemComputing architectures. Molecular logic circuits have been proposed with technologies such as Molecular Field-Effect Transistors (MolFET) and Molecular Field-Coupled Nanocomputing (MolFCN) [7]–[9]. In contrast, only a few molecular devices have been investigated to realize memories [10], [11].

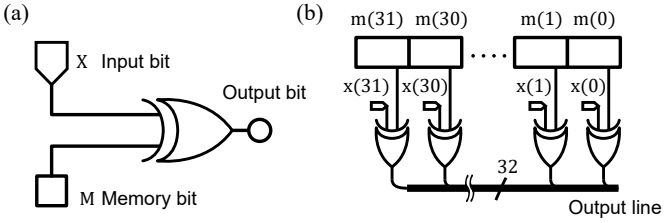


Fig. 1. (a) Basic MemComputing cell. (b) MemComputing array

While technology advances rapidly to implement molecular control [12], molecular device fabrication is still in its infancy. Nevertheless, the scientific community pushes toward realizing molecular devices [13], and a few molecular devices have already been proposed [14], [15]. In contrast, the analysis methods are mature enough to study novel computing architectures. This work demonstrates that molecular phenomena can be exploited to create single-molecule memories. We present two concepts based on the endohedral fullerene and the 6-(Ferrocenyl)hexanethiol (FcC6SH). We demonstrate with *ab initio* calculation that both molecules may encode information in the geometrical and electronic properties of the molecules. The results motivate further research in integrating proposed memories with molecular computing devices and standard CMOS technologies.

II. Methodology

Endohedral fullerenes, indicated as X@C_n, are formed of an element X encapsulated in a fullerene cage C_n, possibly fabricated, e.g., with molecular surgery [16]. We consider the T_d conformation of the C_{28} fullerene since it is the smallest and most stable one at room temperature [17]. We optimize with QuantumATK [18] (v. S-2021.06-SP2) several geometries of the C_{28} with several elements (X) in the cage center to select the most stable (X@C_{28}). We use DFT method with GGA, PBE functional, DZP basis set and with D2 correction [19], [20]. We calculate the X@C_{28} self-consistent total energies E_{tot}, and we select the most stable one (lowest E_{tot}).

To serve as a molecular memory, the most stable X@C_{28} should encode binary information in the X atom position in the C_{28} cage. Therefore, starting from literature initial guesses

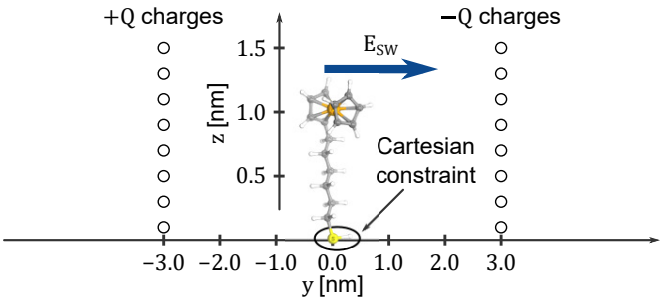


Fig. 2. System used to study the 6-(Ferrocenyl)hexanethiol cation under the influence of an external switching electric field (E_{sw}) generated by positive and negative point charges. The -SH group is constrained in the geometry optimization procedure to emulate the anchoring of the molecule with a possible substrate.

[21], we find the two most stable positions of the X atom inside the C_{28} cage, that we indicate with I-X@C_{28} and II-X@C_{28} corresponding to logic 0 and 1, respectively. Then, we analyze I-X@C_{28} and II-X@C_{28} by calculating their Mulliken Atomic Charge (MAC), and Electron Localization function (ELF) [22], [23]. We express the MAC as an electric charge normalized to the elementary charge e. The ELF is a $\mathbb{R}^3 \rightarrow \mathbb{R}$ function, with a value between 0 (free electron) and 1 (localized electron). We calculate the encapsulation energy E_{enc}:

$$E_{enc,i} = E_{i-X@C28} - (E_{C28} + E_X) \quad (1)$$

where E_X and E_{C28} are is the E_{tot} of the isolated X atom, and isolated C28, respectively, and the $E_{i-X@C28}$ with i=I, II, are the I-X@C_{28} and II-X@C_{28} E_{tot}. Finally, we suppose to read the position-based molecular memory through its dipole moment. The reading operation differs from literature-proposed molecular memory devices, in which the reading operation is usually performed by measuring the current in the two states. Nevertheless, to monitor the memory cell current, electrical contacts are needed, with the difficulty of technological fabrication at the nanoscale. The advantage of our proposal is that contacts should be used only as chip I/O, while internal logic and memory operations may rely on purely molecular devices with real nanometric size. We thus optimize I-X@C_{28} and II-X@C_{28} geometries with refined computational chemistry methods to accurately calculate their dipole moments. We employ DFT/UKS method with ORCA [24], [25] with the B3LYP functional, def2-TZVP basis set [26], and the D3 correction [27], [28]. The same computational method is also used to determine the FcC6SH cation geometry.

To implement the FcC6SH memory cell, one can imagine the cation anchored on a gold substrate through S-Au covalent bonding, e.g. by creating a Self-Assembled Monolayers [29], and we hypothesize the application of electric fields force the molecule to bend on the substrate. The binary information corresponds thus to the FcC6SH bending direction.

We use Constrained Optimization (COPT) on the system schematically depicted in Fig. 2. The -SH group is constrained on the cartesian coordinates to emulate the molecule anchoring. Following the procedure reported in [30], we generate an electric field by positioning the molecule within sixteen point charges (Q_i) with absolute value $|Q_i|$=0.4e at a distance of 3 nm from the molecule. The field at any space point can be precisely calculated with electrostatic equations. For a rough estimation, denoting with ε_0 the vacuum permittivity, the switching field (E_{sw}) can be calculated as:

$$E_{sw} = \frac{1}{4\pi\varepsilon_0} \frac{16 \times |Q_i|}{(3 \times 10^{-9})^2} \approx 1 \text{ V/nm}$$

We also exploit the Aggregated Charge (AC) definition to analyze molecule electrostatics [9]. First, we exploit the CHELPG paradigm [31] to evaluate the atomic charges, normalized w.r.t. e, by fitting the *ab initio* electrostatic potential. Then, we obtained the AC by individually summing the atomic charges of the ferrocene and the hexanethiol.

TABLE I
TOTAL ENERGY FOR VARIOUS ENCAPSULATED ELEMENTS.

geometry	E_{tot} (eV)	geometry	E_{tot} (eV)
Be@C_{28}	-4933.90	Br@C_{28}	-4969.89
Ca@C_{28}	-5609.16	Cl@C_{28}	-4991.11
F@C_{28}	-5223.35	Hf@C_{28}	-6093.40
K@C_{28}	-5367.89	Li@C_{28}	-4753.32
Mg@C_{28}	-6172.00	Na@C_{28}	-5799.48
Rb@C_{28}	-5280.86	S@C_{28}	-4846.42
Zr@C_{28}	-5936.24	Ti@C_{28}	-6177.1
I-Ti@C_{28}	-6177.841	II-Ti@C_{28}	-6177.109

III. RESULTS

A. The endohedral C_{28}

TABLE I reports the E_{tot} of the considered X@C_{28} configurations. The most stable configuration is the Ti@C_{28}, thus we choose it to realize the molecular memory. We find two stable positions of the Ti atom inside the C_{28}

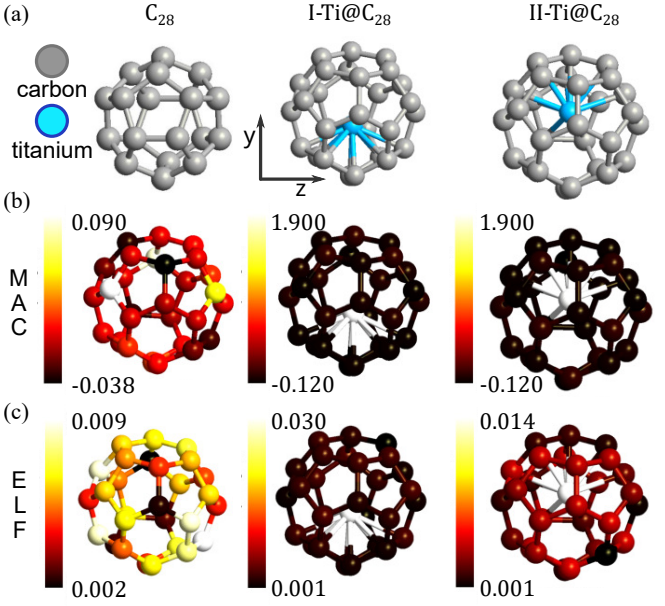


Fig. 3. Optimized geometries (a), MAC (b) and ELF (c) analyses for isolated C_{28}, I-Ti@C_{28} and II-Ti@C_{28}.

TABLE II
DIPOLE MOMENT OF THE I-Ti@C_{28} AND II-Ti@C_{28}.

geometry	μ_x (a.u.)	μ_y (a.u.)	μ_z (a.u.)
I-Ti@C_{28}	0.36837	-1.14476	-0.06499
II-Ti@C_{28}	0.92062	0.77307	-0.05983

cage, named I-Ti@C_{28} and II-Ti@C_{28}. Their total energies are still lower than the other X@C_{28} ones - TABLE I. I-Ti@C_{28} and II-Ti@C_{28} differ by and energy of 732 meV. At room temperature ($\sim$ 300 K) we expect energy fluctuations of the order of $k_BT \sim 26\,\text{meV} \ll 732\,\text{meV}$ (k_B is the Boltzmann constant and T the temperature), thus Ti@C_{28} can be considered temperature-robust at room temperature.

Fig 3(a) reports the C_{28}, the I-Ti@C_{28} and the II-Ti@C_{28} geometries. It is interesting noticing that I-Ti@C_{28} and II-Ti@C_{28} are quite symmetric. The encapsulation energies are respectively: $E_{enc,I} = -8.12\,\text{eV}$ and $E_{enc,II} = -8.05\,\text{eV}$. Such energy values are typical of covalent bonds, indicating a strong chemical interaction between the Ti atom and the C_{28} cage in both cases. Interestingly, $E_{enc,I}$ and $E_{enc,II}$ are lower than the Cr@C_{28} ones obtained in our previous work [32], meaning that the Ti atom has a more marked stabilizing effect on the C_{28} than the Cr. Fig. 3(b) reports the MAC analysis. The Ti atom is slightly positively charged, while the C_{28} cage is slightly negatively charged w.r.t. isolated C_{28}. Thus the Ti atom acts as an electron donor. The ELF analysis in Fig. 3(c) shows that the Ti donated charge is uniformly distributed over the C_{28} cage. Indeed, greater electron delocalization is present in the C_{28} cage in both the I-Ti@C_{28} and the II-Ti@C_{28} compared to the isolated C_{28}.

TABLE II reports the dipole moments of I-Ti@C_{28} and II-Ti@C_{28}. They are similar in magnitude (1.20432 for I-Ti@C_{28} vs. 1.20364 for II-Ti@C_{28}), but the y component changes its direction, meaning they are reversed in direction.

Fig. 4 reports the Ti@C_{28} molecular memory operating principle. At room temperature, there is no spontaneous transition between I-Ti@C_{28} and II-Ti@C_{28}. An extra energy $E_{II\to I}$ should be provided to switch from II-Ti@C_{28} to I-Ti@C_{28}, while and energy $E_{II\to I}$ + 732 meV should be provided to switch from I-Ti@C_{28} to II-Ti@C_{28}. The switching energy can be supplied by an external electric field [11]. The results demonstrate the stable information encoding in the Ti position and corresponding molecular dipole moment. In particular, the dipole moment encoding can generate electric fields that can be used as input for molecular FCN logic devices [33], making MemComputing possible.

TABLE III
DIPOLE MOMENT OF THE 6-(FERROCENYL)HEXANETHIOL CATION

	E_{sw} (V/nm)	μ_x (a.u.)	μ_y (a.u.)	μ_z (a.u.)
FcC6SH	0	-0.29818	0.16191	4.59715
I-FcC6SH	-1	1.64085	-3.82979	2.51510
II-FcC6SH	+1	-1.11990	4.08046	2.41983

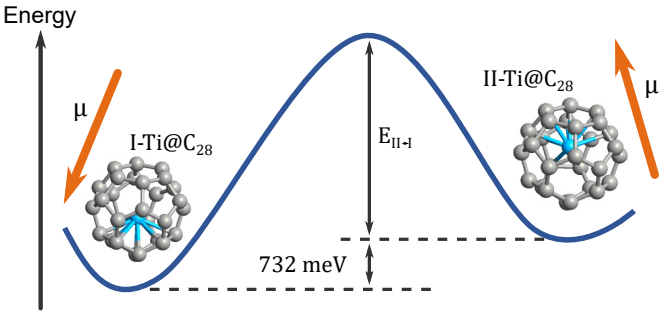


Fig. 4. Operating principle of the Ti@C_{28}-based molecular memory.

B. The 6-(Ferrocenyl)hexanethiol cation

Fig. 5 reports the FcC6SH cation equilibrium geometry obtained through geometry optimization. A single-point calculation provides energy $E_{tot} = -62\,160.46\,\text{eV}$ and dipole moment μ =4.60965 a.u.. TABLE III reports the dipole moment components. A clear polarity of the molecule on the z-axis highlights a charge localization in the ferrocene. As a confirmation, the evaluated ferrocene AC is 0.9581. Considering the cationic nature of the molecule (i.e. normalized total charge +1), the AC analysis denotes a charge aggregation in the ferrocene. When exposed to an electric field, we expect the ferrocene will play a crucial role in the molecule dynamics. On the contrary, the alkyl chain (AC is 0.0419) can be seen as a rigid link between the electrostatically active ferrocene and the substrate.

Fig. 5 shows the results of the COPT calculation with positive and negative switching fields (E_{SW}). As expected, the field acts on the molecule by pushing the electrostatically charged ferrocene in the E_{SW} direction. In addition, the cartesian constraint emulating the anchoring of the molecule forces the FcC6SH cation to bend in the E_{SW} direction. The two bent configurations encode binary information. When the ferrocene bends along the $-y$ direction, the configu ration is named I-FcC6SH, and the cation encodes logic '0'. Contrarily, the II-FcC6SH configuration, with ferrocene bending along the $+y$ axis, encodes logic '1'. TABLE III reports the dipole moment in all the evaluated configurations. The dipole moment y component (μ_y) is consistent with the field direction. Therefore, the logic information is encoded both in

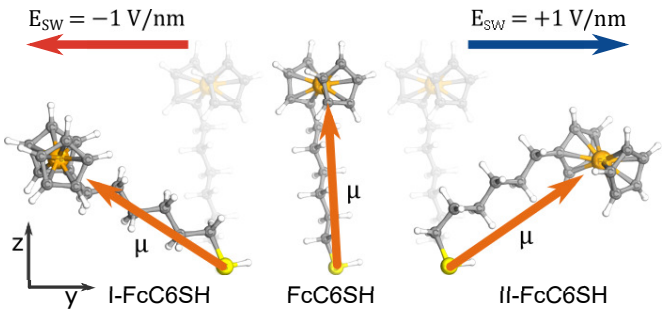


Fig. 5. Geometry of the 6-(Ferrocenyl)hexanethiol when exposed to positive and negative 1 V/nm switching electric fields (E_{sw}). The cation bends in two directions. The bending direction encodes logic information.

the bending of the molecule and in the dipole moment, confirming the expectations. Also, the dipole moment encoding can be eventually exploited to interface with molecular FCN logic devices [33] and enable MemComputing.

Notice that, in this calculation, the substrate is emulated and not explicitly considered. It is possible to verify experimentally that the FcC6SH generally lies on the substrate [29]. Therefore, if the molecule is exposed to the electric field, the substrate accentuates the bending. The molecule will lie on the substrate in ideal conditions when the electric field is switched off, providing non-volatile memory capabilities.

IV. Conclusion

We demonstrate the capability of endohedral $Ti@C_{28}$ fullerenes and 6-(Ferrocenyl)hexanethiol cation to store logic information. Both molecules provide binary encoding through two stable states distinguishable in geometry and dipole moment and are promising for realizing miniaturized molecular memories. The write operation can be performed through the application of external electric fields. Since the information is encoded with stable geometries (at room temperature), the proposed molecules are also suitable for implementing non-volatile memories. The read operation is supposed to be dipole-based by reading the generated electric fields. In this way, the stored logic state can be used as input for molecular FCN circuits, which can perform logic operations, thus completing the MemComputing architectures. The obtained results motivate further research on the integration with molecular FCN circuits, which is here avoided for brevity and since considered out of the scope of this work.

References

[1] F. Mo, C. E. Spano, Y. Ardesi, G. Piccinini, and M. Graziano, "Beyond-cmos artificial neuron: A simulation- based exploration of the molecular-fet," *IEEE Transactions on Nanotechnology*, vol. 20, pp. 903–911, 2021.

[2] Y. Ardesi, A. Gaeta, G. Beretta, G. Piccinini, and M. Graziano, "Ab initio molecular dynamics simulations of field-coupled nanocomputing molecules," *Journal of Integrated Circuits and Systems*, vol. 16, no. 1, pp. 1–8, 2021.

[3] F. L. Traversa and M. Di Ventra, "Universal memcomputing machines," *IEEE Transactions on Neural Networks and Learning Systems*, vol. 26, no. 11, pp. 2702–2715, 2015.

[4] D. Pala *et al.*, "Logic-in-memory architecture made real," in *2015 IEEE International Symposium on Circuits and Systems (ISCAS)*, 2015, pp. 1542–1545.

[5] G. Santoro, G. Turvani, and M. Graziano, "New logic-in-memory paradigms: An architectural and technological perspective," *Micromachines*, vol. 10, no. 6, 2019.

[6] A. Coluccio, M. Vacca, and G. Turvani, "Logic-in-memory computation: Is it worth it? a binary neural network case study," *Journal of Low Power Electronics and Applications*, vol. 10, no. 1, 2020.

[7] H. Fu *et al.*, "Recent progress in single-molecule transistors: their designs, mechanisms and applications," *J. Mater. Chem. C*, vol. 10, pp. 2375–2389, 2022.

[8] C. S. Lent, B. Isaksen, and M. Lieberman, "Molecular quantum-dot cellular automata," *Journal of the American Chemical Society*, vol. 125, no. 4, pp. 1056–1063, 2003.

[9] Y. Ardesi, A. Pulimeno, M. Graziano, F. Riente, and G. Piccinini, "Effectiveness of molecules for quantum cellular automata as computing devices," *Journal of Low Power Electronics and Applications*, vol. 8, no. 3, p. 24, 2018.

[10] B. Daly *et al.*, "Molecular memory with downstream logic processing exemplified by switchable and self-indicating guest capture and release," *Nature Communications*, vol. 10, no. 1, p. 49, Jan 2019.

[11] J. Li *et al.*, "Room-temperature logic-in-memory operations in single-metallofullerene devices," *Nature Materials*, vol. 21, no. 8, pp. 917–923, Aug 2022.

[12] N. Kocić *et al.*, "Implementing functionality in molecular self-assembled monolayers," *Nano Letters*, vol. 19, no. 5, pp. 2750–2757, 2019, pMID: 30933563. [Online]. Available: https://doi.org/10.1021/acs.nanolett.8b03960

[13] Y. Zhao *et al.*, "The fabrication, characterization and functionalization in molecular electronics," *International Journal of Extreme Manufacturing*, vol. 4, no. 2, p. 022003, jun 2022. [Online]. Available: https://dx.doi.org/10.1088/2631-7990/ac5f78

[14] Q. Xu, G. Scuri, C. Mathewson, P. Kim, C. Nuckolls, and D. Bouilly, "Single electron transistor with single aromatic ring molecule covalently connected to graphene nanogaps," *Nano Letters*, vol. 17, no. 9, pp. 5335–5341, Sep 2017.

[15] V. Dubois *et al.*, "Massively parallel fabrication of crack-defined gold break junctions featuring sub-3 nm gaps for molecular devices," *Nature Communications*, vol. 9, no. 1, p. 3433, 2018.

[16] M. Murata, Y. Murata, and K. Komatsu, "Surgery of fullerenes," *Chem. Commun.*, pp. 6083–6094, 2008.

[17] S. Portmann, J. M. Galbraith, H. F. Schaefer, G. E. Scuseria, and H. P. Lüthi, "Some new structures of C28," *Chem. Phys. Lett.*, vol. 301, no. 1-2, pp. 98–104, Feb. 1999.

[18] S. Smidstrup *et al.*, "Quantumatk: An integrated platform of electronic and atomic-scale modelling tools," *J. Phys: Condens. Matter*, vol. 32, p. 015901, 2020.

[19] ——, "First-principles green's-function method for surface calculations: A pseudopotential localized basis set approach," *Physical Review B*, vol. 96, no. 19, p. 195309, 2017.

[20] S. Grimme, "Semiempirical gga-type density functional constructed with a long-range dispersion correction," *Journal of Computational Chemistry*, vol. 27, no. 15, pp. 1787–1799, 2006.

[21] B. I. Dunlap, O. D. Haeberlen, and N. Roesch, "Asymmetric localization of titanium in carbon molecule (c28)," *The Journal of Physical Chemistry*, vol. 96, no. 23, pp. 9095–9097, Nov 1992.

[22] R. S. Mulliken, "Electronic population analysis on lcao–mo molecular wave functions. i," *The Journal of Chemical Physics*, vol. 23, no. 10, pp. 1833–1840, 1955.

[23] A. D. Becke and K. E. Edgecombe, "A simple measure of electron localization in atomic and molecular systems," *The Journal of Chemical Physics*, vol. 92, no. 9, pp. 5397–5403, 1990.

[24] F. Neese, "The orca program system," *Wiley Interdisciplinary Reviews: Computational Molecular Science*, vol. 2, no. 1, pp. 73–78, 2012.

[25] ——, "Software update: the orca program system, version 4.0," *Wiley Interdisciplinary Reviews: Computational Molecular Science*, vol. 8, no. 1, p. e1327, 2018.

[26] F. Weigend and R. Ahlrichs, "Balanced basis sets of split valence, triple zeta valence and quadruple zeta valence quality for h to rn: Design and assessment of accuracy," *Physical Chemistry Chemical Physics*, vol. 7, no. 18, p. 3297, 2005.

[27] S. Grimme, J. Antony, S. Ehrlich, and H. Krieg, "A consistent and accurate ab initio parametrization of density functional dispersion correction (dft-d) for the 94 elements h-pu," *The Journal of Chemical Physics*, vol. 132, no. 15, p. 154104, 2010.

[28] S. Grimme, S. Ehrlich, and L. Goerigk, "Effect of the damping function in dispersion corrected density functional theory," *Journal of Computational Chemistry*, vol. 32, no. 7, pp. 1456–1465, 2011.

[29] F. Schreiber, "Structure and growth of self-assembling monolayers," *Progress in Surface Science*, vol. 65, no. 5, pp. 151–257, 2000.

[30] Y. Ardesi, M. Graziano, and G. Piccinini, "A model for the evaluation of monostable molecule signal energy in molecular field-coupled nanocomputing," *Journal of Low Power Electronics and Applications*, vol. 12, no. 1, 2022.

[31] C. M. Breneman and K. B. Wiberg, "Determining atom-centered monopoles from molecular electrostatic potentials. the need for high sampling density in formamide conformational analysis," *Journal of Computational Chemistry*, vol. 11, no. 3, pp. 361–373, 1990.

[32] C. E. Spano, F. Mo, Y. Ardesi, M. R. Roch, G. Piccinini, and M. Graziano, "Electronic transport study of bistable cr@c28 single-molecule device for high-density data storage applications," in *Proceedings of the 8th World Congress on New Technologies (NewTech'22)*, vol. ICNFA, no. 138, 2022, pp. 138–1 138–9.

[33] A. Pulimeno, M. Graziano, C. Abrardi, D. Demarchi, and G. Piccinini, "Molecular qca: A write-in system based on electric fields," in *The 4th IEEE International NanoElectronics Conference*, 2011, pp. 1–2.